Analysis of ECE Diagnostic for W7-X Stellarator

N.B. Marushchenko, A. Dinklage, H. Hartfuß, M. Hirsch,
H. Maaßberg, Yu. Turkin

Max-Plank-Institut für Plasmaphysik, EURATOM-Association,
TI Greifswald, Germany

Abstract. Accuracy and abilities of the ECE diagnostic system planned to be installed in the W7-X stellarator are analysed with help of ray-tracing simulations. For the expected plasma parameters, the spatial resolution of the standard low-field-side (LFS) X2-mode observation scheme is estimated to be sufficiently high, about 5%. Apart from the LFS scheme, the applicability of other complementary schemes is analysed, in particular, high-field-side (HFS) observation. It is shown, that, in combination with the LFS scheme, the HFS scheme can be quite informative for the problem of distinguishing thermal and non-thermal contributions in the ECE spectrum.

Email: nikolai.marushchenko@ipp.mpg.de

INTRODUCTION

The interpretation of diagnostic data at the W7-X stellarator (under construction in Greifswald, Germany) will be supported by the concept of integrated data analysis [1]. The basic idea is to fit the measured spectral intensity, I_ω, simulated by modeling the data (the antenna, the receiver, *etc*) for a T_e profile. However, one needs to estimate non-thermal contributions in the ECE spectrum, and to find possibilities to extract from measurements the information about these non-thermal effects. Analysis of the capabilities of the ECE diagnostic system, which will be installed at the W7-X stellarator is the main goals of the present work.

In the initial stage, W7-X will operate in the $10^{19}\mathrm{m}^{-3}$ range of densities, with strong ECR heating (up to 10 MW) by X2-mode at 140 GHz. The expected electron temperature range (supported by transport simulations [2]) is 3 - 10 keV. For a highly localized deposition profile, one can expect the appearance of supra-thermal electrons.

The standard scheme of ECE measurements at the 2nd harmonic X-mode is based on i) a good (spatial) localization of the "emission line", and ii) a Maxwellian electron distribution function. While for the appropriate frequency range the first condition is well satisfied (the ECE diagnostic system is planned to be installed near the "bean-shaped" plane, where ∇B is largest), the second one can be violated, especially for low density ECR heated plasmas. Nevertheless, in the LFS observation scheme, the main contribution in the emission is usually produced by the bulk electrons with energies of not more than roughly $2T_e$, i.e. the ECE spectrum is close to the thermal one.

The detection of non-thermal effects requires a special technique. A HFS observation, especially along the LFS sightline [3], appears to be very promising: despite the moderate spatial resolution of a HFS ECE diagnostic, the existence of supra-thermal

electrons can be identified by comparison of both LFS and HFS ECE spectra. Abilities of a HFS diagnostic have been examined both theoretically and experimentally [4], where the high sensibility of the non-thermal ECE is confirmed. Nevertheless, the interpretation of the HFS measurements is not trivial and requires special attention.

RESULTS OF RAY-TRACING SIMULATIONS

The ECE spectrum and its spatial resolution are calculated by a newly developed ray-tracing code, which operates with magnetic field configurations obtained from VMEC calculations. For the simulations, the so-called W7-X "standard" vacuum configuration was used. The absorption coefficient and the emissivity are defined in the general formulation (see, e.g. [5]), by the anti-Hermitian part of the dielectric tensor and the micro-current correlation tensor, respectively. Both these tensors are calculated by integration of the arbitrary fully relativistic electron distribution function. In the code, the contributions of the (ripple-) trapped and passing electrons are calculated separately. The last tool is very useful for stellarator-specific problems, where the different classes of electrons have to be taken into account. The polarization vectors and the power flux are defined with the traditional weakly relativistic dielectric tensor. This model is quite general and covers completely the relevant parameter range.

The electron radiative temperature, T_{ece}, for a frequency $\omega_i = 2\pi f_i$, is calculated as

$$T_{ece}(\omega_i) = \left\langle \frac{8\pi^3 c^2}{\omega^2}\, g(\omega) \sum_{\text{rays}} w_{\text{ray}} \int_{s_0}^{s_1} \mathrm{d}s'\, \eta_\omega(s')\, \mathrm{e}^{-(\tau_\omega(s_1)-\tau_\omega(s'))} \right\rangle_{\omega_i \pm \Delta\omega/2} ,$$

where η_ω and τ_ω are emissivity and optical depth, respectively. The antenna beam is discretized by the number of rays, and the ray weight factor, w_{ray}, being the antenna beam Gaussian pattern, describes the radiation intensity distribution in the beam. For each frequency, ω_i, the results are averaged over the $\omega_i \pm \Delta\omega/2$ range with the correspondent frequency band function, $g(\omega)$, which is the radiometer characteristic (it has been assumed rectangular for each frequency channel). Multiple reflections are not taken into account since it is expected that the torus will be covered by B_4C to strongly increase the wall absorption and to decrease ECRH stray radiation.

The problem of "mapping" the ECE spectrum onto the proper magnetic surfaces also requests special attention. Due to the relativistic and Doppler broadening, a non-locality of the emission line arises, when the gradients of density and temperature can also be important. Instead of the "cold" resonance position, $\mathbf{X}_{cy}$ for a given frequency, one needs to find the "weighted" center of the emission line, $\mathbf{X}_{ece}$, and to estimate its spatial width, ΔX_{ece}, (i.e. the spatial resolution). For the calculations, the same algorithm as in [6] is used: the point at the sightline, where half of the integral emission intensity is reached, is called the center of the (asymmetric) emission line. Finally, the "weighted" center of the emission line, $\mathbf{X}_{ece}$, together with its wings are mapped onto

the magnetic coordinates, producing $r_{\rm eff}(\mathbf{X}_{ece})$ and the appropriate "error bars".

The aim of this work is to estimate the contribution of the supra-thermal electrons in ECE. In principle, in order to study this effect in details, Fokker-Planck simulations are required. But for preliminary estimations (without looking to any concrete scenario), it is sufficient to use the simplified bi-Maxwellian model. The electron distribution function is represented as $f_e = (1-\delta)f_0 + \delta f_1$, with f_0 and f_1 being Maxwellian distribution functions, the main one and the supra-thermal one, respectively. For the highly localized ECRH deposition profile, it is also assumed, that the supra-thermal fraction exists only near the axis, $r_{\rm eff} \lesssim 5$ cm, with a Gaussian shapes of its weight and its temperature. Axial values are $\delta(0) = 0.05$ and $T_{e1}(0)/T_{e0}(0) = 3$, which correspond to 15% of the energy contained in supra-thermal electrons in the plasma center. Despite its crudeness, this model is more or less adequate to the expected quasi-linear flattening of the electron distribution function, producing a non-negligible supra-thermal fraction in the most interesting range, $v/v_{th} \approx 1.5-3$ with $v_{th} = (2T_e/m)^{1/2}$. Simulations are performed for $n_e(0) = 2\cdot 10^{19}$ m^{-3} with an almost flat profile near the axis (within the heated region), and for a peaked T_e profile with $T_e(0) = 5$ keV. The magnetic field on axis at the "bean-shaped" plane is taken to be $B = 2.5$ T.

It is assumed, that the antenna has a thin cone of divergence, 1.2°, and the beam cross-section size at the antenna is equal 1 cm. All frequency channels are assumed to have the band width of $\Delta f = 0.35$ GHz. The poloidal and toroidal angles of the LFS observation are chosen i) to see the axis, and, ii) to minimize the values of $N_\parallel$ along the sightline, keeping, in particular, $N_\parallel(r_{\rm eff} = 0) \simeq 0$. The HFS antenna is assumed to be located at the opposite position. For operation at moderate densities, the refraction effects are almost negligible, and both sightlines should coincide. For the chosen sightlines, mainly the passing electrons are seen by the ECE antennae, and the total fraction of trapped electrons contributing to the ECE is less than 15%.

For $B = 2.5$ T, the magnetic field varies along the ECE observation chord between 2.25 T and 2.82 T, and the frequencies for the 2nd and 3rd harmonics have no overlap (from 126 GHz to 158 GHz and from 189 GHz to 237 GHz, respectively). The frequency range from 115 GHz to 220 GHz, used for the simulations, covers both the 2nd and the 3rd harmonics ranges. The lower frequency limit (2nd harmonic) is chosen to cover the down-shifted emission from the supra-thermal electrons for both LFS and HFS cases. The 3rd harmonic range is discussed below. For comparison, in Fig. 1 both the LFS and the HFS ECE spectra are shown.

Let us first analyse the 2nd harmonic range. Excluding the low-frequencies ($f < 127$ GHz), for which the plasma is optically thin, the LFS spectra does not show any significant difference between the thermal and the non-thermal ones. However, the HFS spectrum has a well pronounced peak at low frequencies, indicating the contribution of the supra-thermal electrons. Despite the fact, that for these frequencies the "cold" resonance position, $\omega = 2\omega_{ce}$, is far from the axis (and may be even outside of the plasma), the "weighted" center of the emission line, being observed from HFS,

is located near the axis. This is clearly seen in Fig. 2 (left), where the emission line profiles at $f = 128$ GHz for both cases are shown. The chosen frequency corresponds

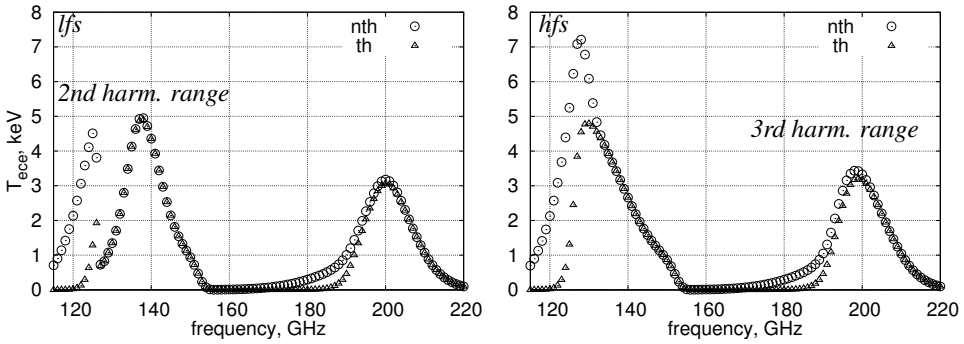

Figure 1. ECE spectrum (radiative temperature, T_{ece}) for LFS (left) and for HFS (right) observations near the "bean shaped" plane; $\triangle$ - thermal spectrum, $\circ$ - bi-Maxwellian spectrum.

to the top of the HFS spectrum. One can see, that due to strong reabsorption, the emission observed from the LFS is coming from the region very close to the "cold" resonance position, $R \simeq 6.08$ m, i.e. from the periphery of the plasma. And, vice versa, emission observed by the HFS antenna, originates from the central region of the plasma, $R \simeq 5.9$ m, where the non-thermal population exists. In other words, the down-shifted emission of energetic electrons near the axis, which propagates in the direction of increasing B is not reabsorbed, and can be identified in the measurements. The importance of this difference between the LFS and HFS spectra for the interpretation and for the "mapping" of it onto the radius, is demonstrated in Fig. 2 (right). Here are shown the major radius projections of the weighted center of the emission line, R_{ece}, versus the corresponding "cold" resonance (major radius) position, R_{cy}. As

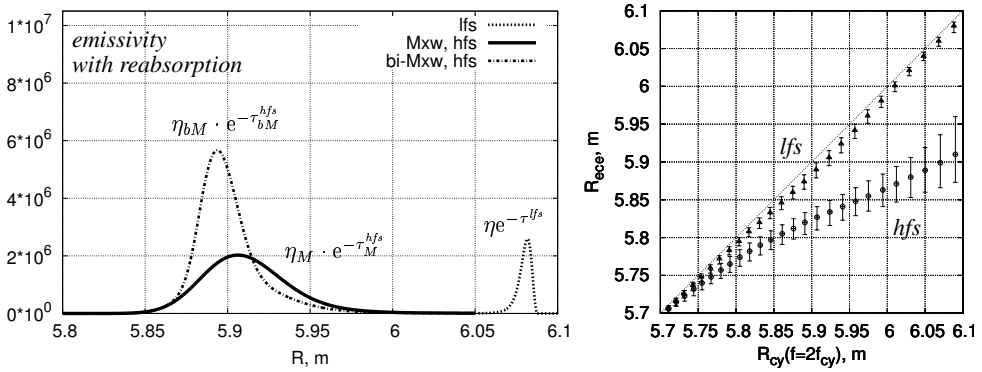

Figure 2. Left: spatial ECE line profiles at 128 GHz. Right: the "weighted" centers of the emission line *vs* the "cold" resonance positions ($\omega = 2\omega_{ce}$).

expected for the LFS spectrum, R_{ece} is very close to R_{cy}, being down-shifted by not more than 2 cm. But the HFS spectrum has R_{ece} strongly shifted below R_{cy} inside the plasma. In fact, the spatial location of the emission line is dominated by reabsorption, and not by emission.

One can compare also the velocities of electrons, which contribute to the emission (Fig. 3, left). Due to the strong reabsorption, the bulk electrons with $v/v_{th} \simeq 1$ are responsible for the LFS ECE spectrum. But for the HFS spectrum, much more energetic electrons contribute to the EC emission, especially in the range 115 GHz $\leq f \leq$ 130 GHz, where only (supra-thermal) tails of the distribution function with $v/v_{th} \sim 3 - 4$ are responsible.

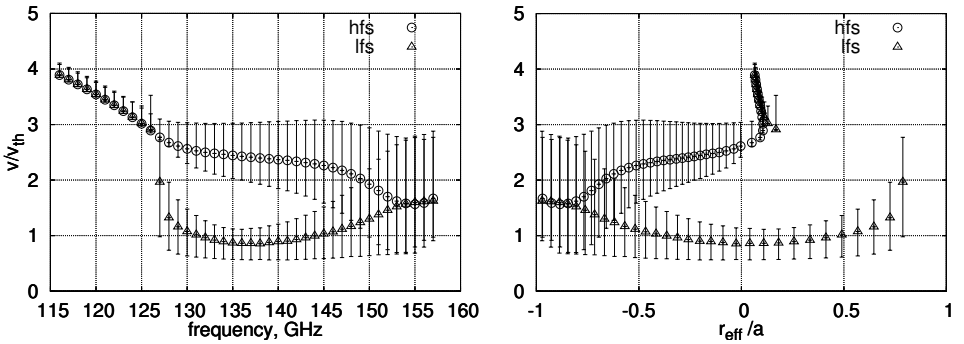

Figure 3. Velocities of emitting electrons as function of frequency (left) and effective radius (right) for the "bean shaped" plane, 2nd harmonic ($\triangle$ - LFS, $\circ$ - HFS).

For another scenario with off-axis non-Maxwellian electrons, the comparison of HFS and LFS should be a powerful tool. In Fig. 3 (right), the velocities of emitting electrons are shown, mapped onto the effective radius (procedure of mapping is described above). Here is clearly seen that the low frequency channels of the HFS observation contain only the information from the central region of the plasma. The HFS measurements do not reproduce the "right hand" part of the $T_{ece}(r_{\rm eff})$ profile, the region $r_{\rm eff} > 0$ is covered only by the LFS observation (see also Fig. 5). Observe also in Fig. 3 (right), that the velocity range of emitting electrons is not symmetric in $r_{\rm eff}$ for both LFS (not strongly pronounced) and HFS cases. For the LFS case, the main reason is that the sightline cannot be perpendicular to the magnetic surfaces everywhere. Also the finite width of the beam and the finite $\Delta\omega$ (both are taken into account) play a non-negligible role.

In Fig. 1 are also shown the other parts of the ECE spectrum, related to the 3rd harmonic, 180 GHz $\leq f \leq$ 220 GHz. Note, that these frequency limits differ from the appropriate "cold" resonance harmonic range. For these frequencies, the optical depth is much smaller, $\tau \simeq 1$, and the spatial resolution is not sufficiently high. As consequence, the 3rd harmonic ECE spectrum is significantly down-shifted for both LFS and HFS observations. Nevertheless, it has diagnostic potential. First of all, both the LFS and the HFS observations give almost the same spectra (contrary to the 2nd harmonic case, they have almost the same velocities of emitting electrons, $v/v_{th} \sim 1.5 - 2$), and they can be used for verification of the 2nd harmonic measurements.

Another promising possibility is the ECE observation in the "triangular" plane, with the inverted ∇B along the sightline. The main advantage is that this HFS observation can be performed using the outer port. The position of the ECE antenna can be chosen

to have a monotonic decrease of B along the sightline with minimized $N_{||}$. The ECE spectrum is qualitatively the same as for the HFS in the "bean-shaped" plane, with down-shifted frequencies corresponding to the lower B. Because of lower $|\nabla B|$, the spatial resolution in the central region is fairly low. Nevertheless, these measurements, having a large contribution of trapped electrons (about 50%), should be very informative, especially for investigations of the (optional) ECCD scenario with launching close to the "triangular" plane. In this scenario (the oblique launch of RF power from the HFS) the power is absorbed by high energetic electrons, and the HFS ECE measurements, respectively, can give the requested information.

SUMMARY

As expected, the standard ECE technique, i.e. the LFS ECE measurements near the "bean-shaped" plane with 2nd harmonic X-mode, is the most accurate and convenient method to obtain the electron temperature profile (the largest width of the emission line is about 2 cm, i.e. the spatial resolution is about 5%).

Additional information, related to non-thermal electrons, can be obtained with complementary HFS measurements in both the "bean shaped" and the "triangular" planes. Apart from simplicity in realization, the "triangular" plane is especially interesting due to the circumstance, that the ripple-trapped electron contribution in the ECE radiation can significantly exceed that from the "bean-shaped" plane. For comparison, in the "triangular" plane of the "standard" configuration the trapped electrons contribution in ECE is about 50%, while near the "bean-shaped" plane it does not exceed 15%. Despite lower spatial resolution, the HFS spectrum (especially its low-frequncy range) contains interpretable information on the non-thermal population of electrons. It has to be stressed also, that the HFS measurements cannot be interpreted without comparison with the standard LFS results.

The 3rd harmonic frequency range might provide sufficient information for all schemes discussed above. Despite the low optical depth, $\tau \simeq 1$, the part of the ECE spectrum with $\omega > 3\omega_{ce}(0)$ has a spatial resolution very similar to the 2nd harmonic HFS spectrum, i.e. T_{ece} is much less than for 2nd harmonic LFS spectrum, but quite suitable for the identification of the emitting region.

References

[1] A. Dinklage, R. Fischer,, J. Svensson, Fusion Sci. Technol. **46** (2004) 355

[2] M. Romé *et al.*, Plasma Phys. Control. Fusion **40** (1998) 511

[3] N.B. Marushchenko *et al.*, 31st EPS Conference Plasma Phys., London, 28 June - 2 July 2004 ECA Vol.**28G**, P-1.204 (2004)

[4] G. Giruzzi, Nuclear Fusion **28** (1988) 1413; J.F.M. van Gelder *et al.*, Plasma Phys. Control. Fusion **40** (1998) 1185; P. Blanchard *et al.*, Plasma Phys. Control. Fusion **44** (2002) 2231

[5] M. Bornatici and F. Engelmann, Phys. Plasmas, **1** (1994) 189

[6] V. Tribaldos and B.P van Milligen, Nuclear Fusion **38** (1996) 283